Fibers and Polymers 2015, Vol.16, No.1, 173-180
DOI 10.1007/s12221-015-0173-z

ISSN 1229-9197 (print version)
ISSN 1875-0052 (electronic version)

Impact Response of Nano Reinforced Mat Glass/Epoxy Laminates

J. A. M. Ferreira[1,2], D. S. C. Santos[2], C. Capela[1,3]*, and J. D. M. Costa[1,2]

[1]*CEMUC, Center of Mechanical Engennering, University of Coimbra, Coimbra, Portugal*
[2]*Mechanical Engineering Department, University of Coimbra, Coimbra, Portugal*
[3]*Mechanical Engineering Department, ESTG, Polytechnic Institute of Leiria, Leiria 2411-901, Portugal*

(Received November 29, 2013; Revised August 27, 2014; Accepted September 1, 2014)

Abstract: The present work intends to characterize the effect that nanoclay and carbon nanotubes matrix reinforcements have on low velocity impact response of epoxy/glass fiber composites. The composite matrix used was the epoxy resin Biresin® CR120 combined with the hardener CH120-3 and the fiberglass triaxial mats ETXT 450. The results of the present paper are discussed in terms of load-time, load-displacement, energy-time diagrams and damage. The incorporation of nanoparticles produces only small improvement of the impact response in terms of the peak load and specific recovery energy. Peak load decreases slightly with increasing percentage of nanoparticles reaching a maximum decrease of 6 % for 3 wt% of nanoclays. Specific recovery energy increases in comparison with control formulation, around 14-18 % for 0.5 wt% addition of nanotubes and 7-15 % for 1 wt% of nanoclays, respectively. Specific recovery energy tends to decrease for higher percentages of nanoparticles in consequence of its poor distribution. Damaged area apparent shows a small reduction with nanoparticle content.

Keywords: Carbon nanotubes, Nanoclays, Glass fiber composites, Impact tests

Introduction

Fiber reinforced laminate composites have been widely used in aerospace, automobile and marine industries, due to their high specific strength and the possibility to obtain optimal material properties in the desired directions. Composite laminates offer an excellent in-plane performance, but have inferior through-thickness properties, particularly in case of impact loads. This is a consequence of manufacturing techniques which do not provide fibers orientated in the thickness direction to sustain transverse load [1], thus reducing the residual strength [2-6].

The optimized design of composites with high impact resistance requires the understanding of how the energy is dissipated in each failure mode. Failure in laminated composites is usually studied using continuum damage mechanics approaches which homogenize material properties studying the damage at the ply/lamina level [7-10]. Micro-mechanics approaches that consider the damage at the constituent level are computationally expensive and require extensive experimental characterization to obtain mechanical parameters to use in the damage models. For example, Nguyen *et al.* [11] used micromechanics-approach to model the debonding process on the interfaces between the inclusions and the matrix and Meraghni *et al.* [12] studied the combined effects of micro-cracks and debonding on the effective properties of a composite. Continuum damage approaches use internal variables to quantify the degradation of elastic properties. For example, Hassan and Batra [13] used three variables to characterize damage due to fiber breakage, matrix cracking and fiber/matrix debonding. Batra *et al.* [14] use a damage evolution criteria proposed by Matzenmiller *et al.* [15], assuming an elastic-plastic behavior of the matrix and an elastic behavior of the fibers.

In recent years, many researchers have explored matrix modification by the addition of different types of nanoparticles, namely, TiO_2, carbon nanofiber, carbon nanotubes and nanoclays to improve mechanical properties. However, reported results of fracture toughness on nanoclay filled composites showed no apparent consensus. Weiping *et al*. [16] studied the performance of epoxy matrix composites and concluded that nanocomposites made with high a pressure mixing method showed fracture toughness K_{1C} and G_{1C} improved by 1.89 and 3.25 times, respectively, even for a low clay content (about 1 wt%) in comparison with pristine resin properties. In contrast, Kornmann *et al.* [17] and Kinloch *et al*. [18] reported that the fracture toughness of the epoxy/clay nanocomposites is lower than that of microcomposite. This may be due to the poor clay dispersion at high concentrations, which results in the formation of big clusters of clay that reduce the plastic deformation of polymer matrix. Dispersion and orientation have a significant role on mechanical properties and particularly on interlaminar fracture strength. Yokozeki *et al.* [19] concluded that the dispersion of cup-stacked carbon nanotubes between fiber mats can delay the onset of matrix cracking of carbon fiber reinforced composites. Literature results suggest that distributing the nanoparticles into resin between layers, preferentially orientated in thickness direction, may improve the IFT of fiber reinforced laminated composites. This beneficial effect was shown by Fan *et al.* [20] in glass/epoxy composites filled with a small quantity of preferentially oriented oxidized multi-walled carbon nanotubes manufactured by a double vacuum assisted resin transfer molding method.

In spite of the abundant literature reporting the mechanical behavior of nanoparticle reinforced matrix polymer composites,

*Corresponding author: ccapela@ipleiria.pt

scarce studies on their impact response were found. Hosur *et al*. [21] studied the low-velocity impact response of sandwich panels manufactured with polyurethane foams reinforced with 0.5 wt% and 1 % wt% of Nanocor® I-28E nanoclay, and concluded that nanoclay infused foam sandwich structures exhibited higher peak loads and smaller damage area than their neat counterparts. Then, by using nanophased sandwich construction it is possible to sustain higher loads, reducing the damage size during impact. Reis *et al*. [22] studied the effect of nanoclays incorporation on the impact-resistance of Kevlar/epoxy laminates and concluded that the samples manufactured with epoxy resin filled by nanoclays showed improved performance in terms of elastic recuperation and penetration threshold. Reis *et al.* [23] studied also the impact behavior on bi-directional glass fibre/epoxy resin composites and concluded also that the introduction of nanoclays promotes significant benefits especially in terms of displacement and elastic recuperation. Crack-pinning is frequently cited as one of the key enhancement mechanisms to improve the mechanical performance by the addition of soft nano-particles [24]. Recently, rigid nano-particles such as carbon nanotubes (CNT) have been used as toughening reinforcements due to their high aspect ratios and excellent mechanical properties. Failure mechanisms of CNT are mainly based on fiber pull-out and fracture. Multi-walled CNT (MWCNT), have been more widely utilized for the development of enhanced laminated [25] due to their low cost, commercial availability in large quantities and ease of dispersion, but single-walled CNT (SWCNT) offer superior performance due to their higher surface areas, higher aspect ratios, more efficient load transfer and better mechanical properties due to higher crystallinity [26]. Ashrafi *et al.* [27] studied the production and characterization of SWCNT-modified carbon fiber/epoxy laminated composites and observed that the incorporation of 0.1 wt% of SWCNT resulted in a 5 % reduction of the area of impact damage and 3.5 % increase in compression-after-impact strength. Venkatanarayanan and Stanley [28] studied the intermediate velocity bullet impact response of hybrid resin with MWCNT in proportions by weight of 0.1-1.0 %) obtaining significant improvement on absorption capability in comparison with epoxy resin.

Saghafi *et al.* [29] studied the effect of interleaved polyvinylidene fluoride (PVDF) nanofibers in glass/epoxy laminates with stacking sequence [0/90/0/90]s concluding that it was not an effective solution to improving impact damage resistance of GFRP.

Much more investigation is needed about impact response of laminates, particularly about the benefits of using hybrid composites. The present work aims to contribute to study the effect of addition of small amounts of nanoparticles in the resin on low velocity impact response of epoxy/glass fiber composites. The results of the present paper are discussed in terms of load-time, load-displacement, energy-time diagrams and damage. The impacted plates have been inspected by ultrasonic techniques in order to quantify damage areas and the residual strength was obtained by tensile tests.

Materials and Testing

Specimens Manufacture

The matrix was the epoxy resin Biresin® CR120, formulated by bisphenol A - (epichlorhydrin) epoxy resin 1,4-bis(2,3-epoxypropoxy) butane, combined with the hardener CH120-3, both supplied by Sika. The matrix was nano enhanced using the organo-montmorillonite nanoclays and MWNT. The laminate plates were processed using 10 layers of fiber glass type E, triaxial mats ETXT 450, supplied by Saapi, with fiber orientation 90 ^{o}/±45 ^{o} balanced with 150 grams/m^2 on each of the three directions. The nanoclay used in this study was commercially available organo-montmorillonite, Nanomer® I30E, surface modified with an octadeyl amine, provided by Nanocor Inc. with an average clay length 9.5 mm, measured by granulemetric laser scattering analysis using a Malvern Mastersizer 2000 equipment. The multiwalled carbon nanotubes (MWNT) have 98 % (wt%) in carbon, with average diameter 6.6 nm and 5 μm length according supplier Sigma-Aldrich.

Both clays and nanotubes were dispersed into the epoxy resin using a direct mixing method. The mixture of resin and the desired amount of nanoparticles was done using high rotation mixing (8,000 rpm) during 1 h. Then, the mixture was degassed under vacuum for 15 minutes and afterwards the hardener agent was added.

Composites were manufactured with five different matrix formulation as indicated in Table 1, wherein the percentages of nanoparticles are aligned with those used in the literature [16-18,22,28]. The specimens tested were machined from plates manufactured by moulding in vacuum. Fibers and resin were hand placed in a mould with all the fibers layers oriented in the same direction and subjected to a compression of about 0.1 MPa. The mould was put into a vacuum bag as shown in Figure 1. To obtain good mould release, a film that promotes the separation between the plate surface and the moulding was used. In the manufacture of the plates, woven fiberglass layer and resin were applied alternately, while ensuring the complete impregnation of the fibers.

The composite laminates were cured at room temperature

Table 1. Formulation of composite matrix and laminate strength

Reference	Epoxy (wt%)	Nanoclay (wt%)	MWNT (wt%)	Tensile strength (MPa)
GF/E	100	-	-	332±21
GF/ENC1	99	1	-	321±18
GF/ENC3	97	3	-	305±16
GF/ENT0.5	99.5	-	0.5	319±5
GF/ENT1	99	-	1	310±15

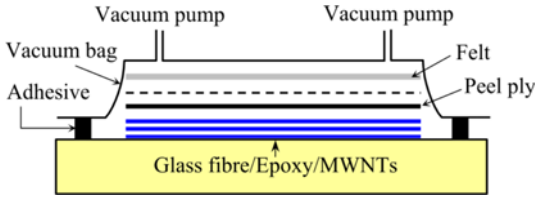

Figure 1. Schematic view of the vacuum bag in mould curing process.

for 8 hours. The resulting plates were 300 mm long, 100 mm wide and nominally 4.2 mm thick. Post cure process was carried out as follows: 55 °C during 16 hours, 75 °C during 3 hours and finally 120 °C during 12 hours.

Impact and Residual Strength Tests

Low-velocity impact tests were performed using a drop weight-testing machine CEAST 9350. Semi-spherical tip impactor with 3.4 kg of mass was used. The tests were performed according to ASTM D3763 standard on square section samples of 100×100 mm and the impactor stroke at the centre of the samples using a circular 75 mm diameter support. The impact energies used in the tests were 8 and 16 J. These energies were previously selected in order to enable the measuring of the damage area, but without promoting perforation of the specimens. For each condition, four specimens were tested at room temperature. After impact tests, a 40×40 mm area centred around the impact point of the specimens was inspected by a C-Scan technique to evaluate the size of the damaged zone. Subsequently, the specimens were cut again to be submitted to tensile tests in order to obtain the residual strength. In this process, a circular diamond saw was used and a very careful procedure was applied, in order not to introduce manufacturing defects. The final dimensions of the specimens were 100×45 mm which includes the area analysed by C-scan. The most usual process of characterizing the residual strength is doing compression tests. However, due to the fact that an anti-buckling system is not available in the laboratory at the moment, the residual resistance was obtained by tensile tests, performed in an electromechanical Instron Universal Testing machine (model 4206), with a displacement rate of 1 mm/min at room temperature.

Results and Discussion

Samples of nano enhanced resin layers were prepared in an ultramicrotome for ultrathin sectioning EM FCS, Leica Company. Morphological analyses were realized in an Ultra-high resolution Field Emission Gun Scanning Electron Microscopy (FEG-SEM), NOVA 200 Nano SEM, FEI Company, using a Scanning Transmission Electron Microscopy (STEM) detector and an acceleration voltage between 15 and 18.4 kV to obtain the micrographs. Figure 2(a)) and

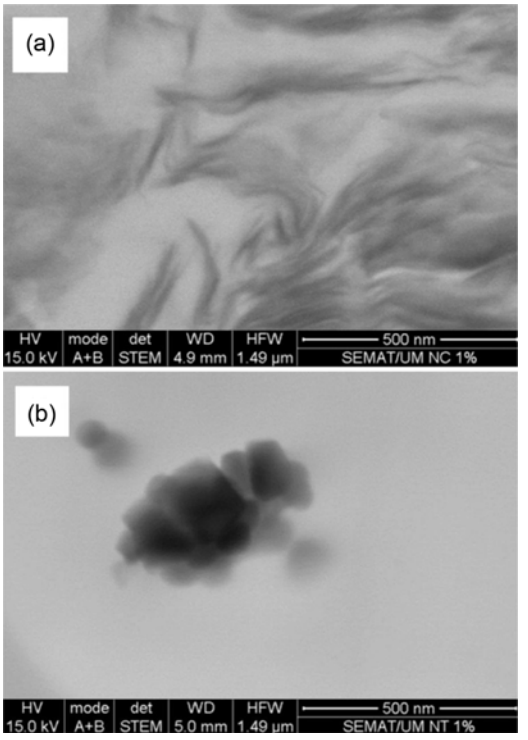

Figure 2. TEM observations of resin interlayer; (a) GF/ENC1 and (b) GF/ENT1.

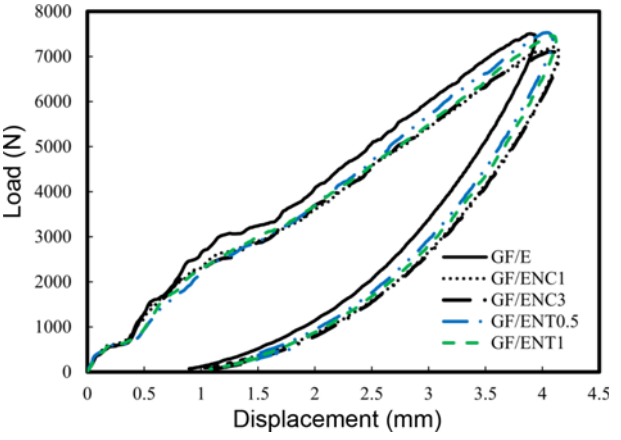

Figure 3. Load versus displacement curves for 16 J incident impact energy.

Figure 2(b)) show two of these observations for 1 % of nanoclay and nanotubes, respectively. Good dispersion, intercalation and clay exfoliation was observed in Figure 2(a) for 1 % nanoclay, while in Figure 2(b) a poor dispersion was obtained with formation of agglomerates.

Tests were carried out with impact velocity of 2.165 and 3.06 m/s, respectively for incident impact energies of 8 and 16 J. The time range for acquisition data was 6 microseconds. Figures 3 and 4 show some typical curves, load versus

displacement and load versus time, respectively, obtained for the five composite architectures and the impact energy of 16 J. These curves are representative of the tests (for the impact energy of 8 J the curves were similar) and show the typical behaviour for composite laminates, characterized by an increase in the load up to a maximum value, P_{max} followed by a drop. In all tests the impactor deforms the specimens and always rebounds, which means that the maximum impact energy was not high enough to produce full penetration. Both figures show small differences between the impact responses of the five composites. However, the maximum impact loads tend to decrease when the nanoparticles are added into matrix.

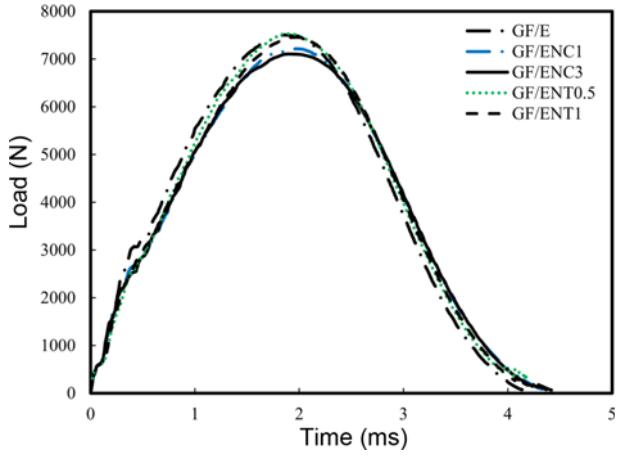

Figure 4. Load versus time curves for 16 J incident impact energy.

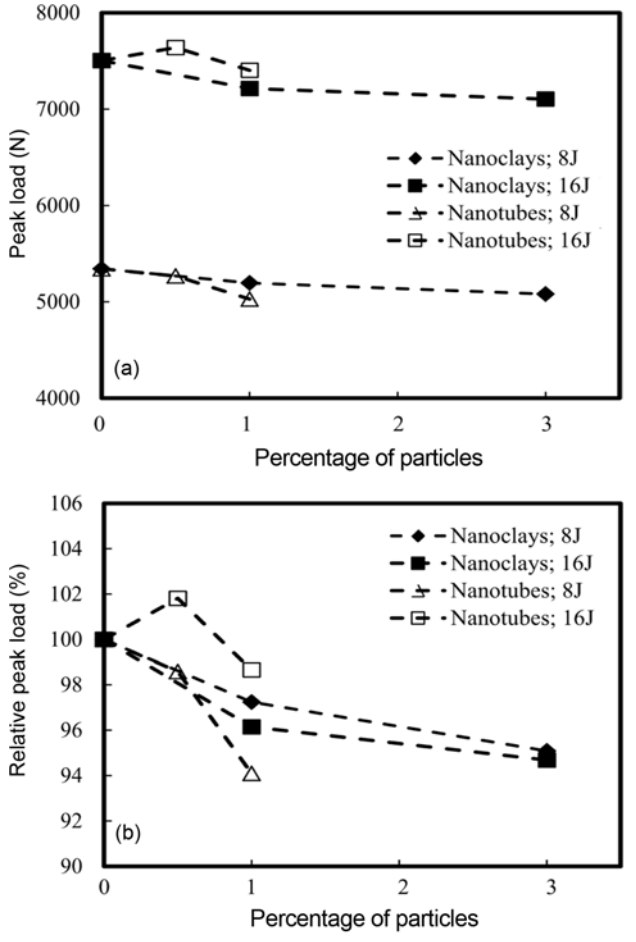

Figure 5. Maximum impact load versus % of particles.

Figure 5(a) shows the average values of the peak load, in terms of absolute values, for each laminate architecture and incident impact energy, against the percentage of nanoparticles. In most cases, small decrease of peak load with the addition of nanoparticles was observed, for both incident impact energies. The analysis of Figure 5(a) is complemented by Figure 5(b), in which the relative peak load in percentage was plotted (calculated as the actual peak/peak load for the reference laminate multiplied by 100) against the percentage of nanoparticles. The analysis of this figure shows small decreasing of peak load with the percentage of particles reaching about 6 % for the higher values of particle content. These results are partially in disagreement with those obtained by Reis *et al.* [22] which get an only marginally peak increase load with the incorporation of nanoclays in Kevlar/epoxy composites. This increase would be expected in consequence of the stiffener promoted by nanoparticles adding. However, Çallıoglu *et al*. [30] obtained significant decrease of peak load on woven glass/polyester-matrix composite plates filled up to 20 % SiCp ceramic particles. The differences in results are related with changes of failure mechanisms, scatter in specimen's thickness. In the present work an average scatter of 2 % on the results of the peak load was obtained, which can be mainly attributed to variations in the thickness of the specimens, whose deviation was within 4.2±0.2 mm. The changes in thickness could

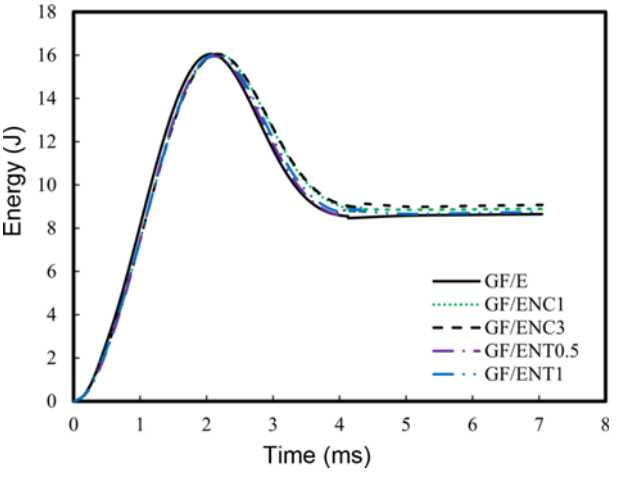

Figure 6. Energy versus time curves for 16 J incident impact energy.

Table 2. Impact response of composite laminate

Reference	Impact energy (J)	Peak load (kN)	Absorbed energy (J)
GF/E	8	5.35±0.07	3.68±0.13
GF/ENC1	8	5.22±0.20	3.5±0.10
GF/ENC3	8	5.10±0.07	3.45±0.15
GF/ENT0.5	8	5.28±0.14	3.4±0.14
GF/ENT1	8	5.04±0.18	3.4±0.15
GF/E	16	7.51±0.19	8.8±0.30
GF/ENC1	16	7.23±0.17	8.75±0.35
GF/ENC3	16	7.11±0.19	8.8±0.23
GF/ENT0.5	16	7.65±0.22	8.3±0.10
GF/ENT1	16	7.41±0.25	8.4±0.34

have a direct relationship with the percentage of particles, since the viscosity of the mixture tends to grow with the number of particles and consequently the thickness of the resin layers between fibers may increase, but in this study the observed variation is random.

Figure 6 shows some typical curves of the energy versus time for 16 J incident impact energy, which are close for all five composites. The lower values of energy on plateau of figures relate to higher elastic recovery and, consequently, lower levels of damage were obtained for the neat matrix (control specimens) and carbon nanotube enhanced matrices. The beginning of the plateau of the curve is coincident with the loss of contact between the striker and the specimen, so, this energy coincides with that absorbed by the specimen.

Table 2 gives the average values and standard deviation of the peak load, absorbed energy for each laminate impacted at both incident impact energy levels. The elastic recovery energy was calculated as the difference between the absorbed energy and the energy at peak load.

Absorbed and elastic recovery energies were also calculated in terms of percentage of the incident impact energy. Figure 7 shows the average values of the absorbed energy against the percentage of nanoparticles. The percentage of absorbed energy increases significantly (about 10 % of impact energy) when the impact energy is increased from 8 J to 16 J for all laminate architectures, which means that impact energy of 16 J produces a significantly greater damage than 8 J. This preliminary conclusion will be confirmed later, once to the incident impact energy of 16 J will occur larger damaged areas and smaller values of residual strength. Carbon nanotubes enhanced matrix composites absorb an energy 3-4 % lower than control samples. For nanoclay enhanced matrix laminates the absorbed energy also decreases slightly (about 3 %) in comparison with control composite for 8 J impact energy, but remains nearly constant for 16 J impact energy, indicating a reduced efficiency of nanoclay filling to enhance impact response for higher values of incident impact energy, which agree with the results obtained by Reis *et al*. [22] on Kevlar/epoxy composites.

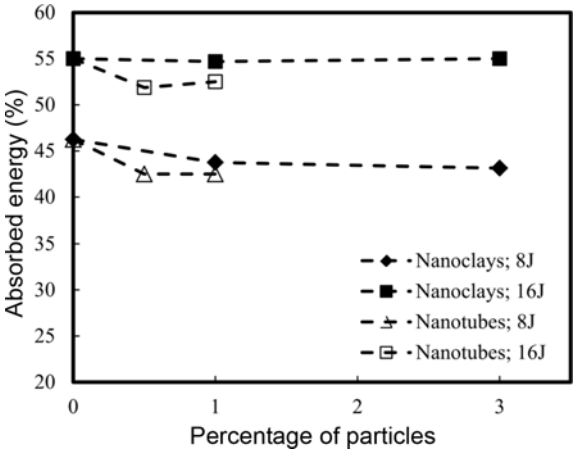

Figure 7. Absorbed energy versus % of particles.

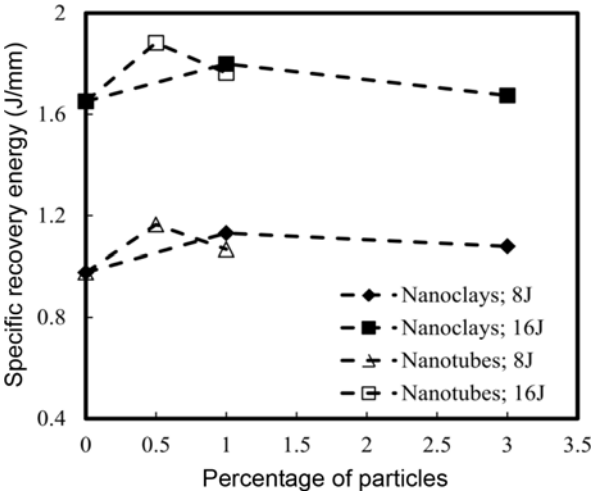

Figure 8. Specific recovery energy versus % of particles.

Recovery energy presents, obviously, an inverse tendency of that drawn in Figure 7, i.e. for carbon nanotubes enhanced matrix composites the recovery energy is about 3-4 % higher than control samples and for nanoclay enhanced matrix laminates it is also higher about 3 % for 8 J, but remains nearly constant for 16 J impact energy. The results in Figure 7 indicate the current values obtained from the tests and don't take into account the normal fluctuations in specimen's thickness. In order to consider the thickness effect, the specific recovery energy (recovery energy divided by specimen thickness was calculated. Figure 8 shows the average values of the specific recovery energy against the percentage of nanoparticles. The analysis of this figure reveals that significant gains were obtained for all composite laminates incorporating enhanced matrices. As example, for 8 J impact energy the specific recovery energy increases about 18 % and 15 % for 0.5 % wt of nanotubes and 1 % of nanoclays, respectively. However, for 16 J impact energy the gain is

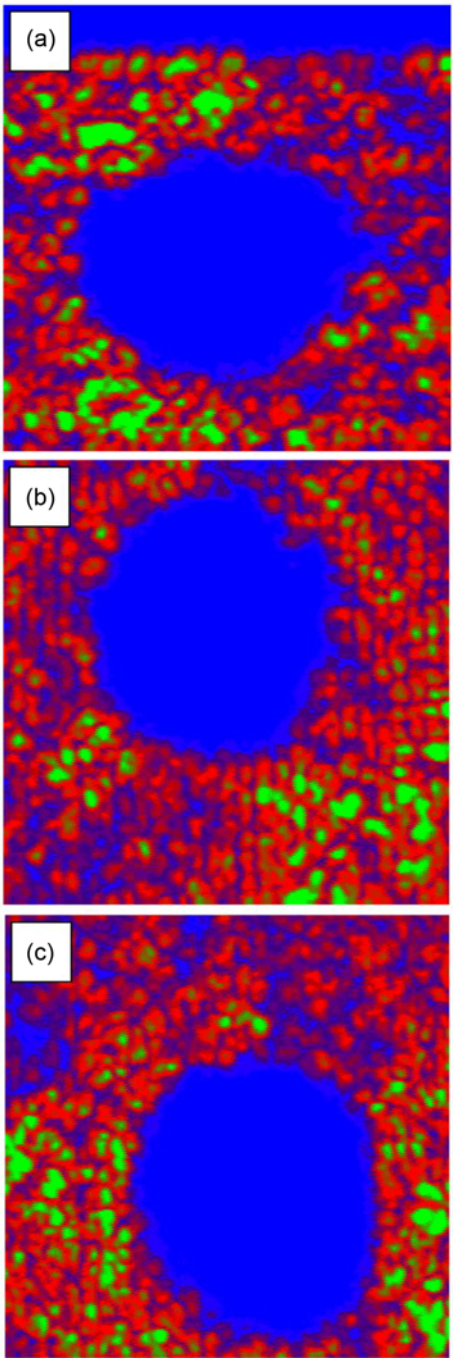

Figure 9. C-scan observations of damaged area; (a) GF/E specimen, (b) GF/ENT0.5 specimen, and (c) GF/ENT1 specimen.

lower, of about 14 % and 7 % for 0.5 % wt of nanotubes and 1 % of nanoclays, respectively. The gain of the specific recovery energy decreases with higher percentages of nanoparticles because in those cases a poor distribution of the particles was achieved.

Samples impacted with 16 J were inspected by C-Scan technique in a square area of 40×40 mm, containing the

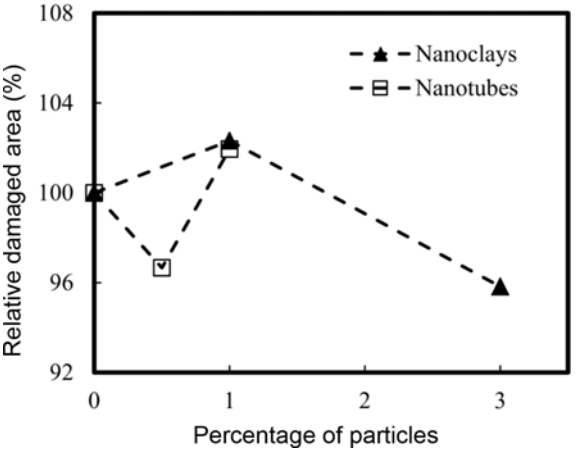

Figure 10. C scanned damaged area versus % of particles for 16 J impact energy.

impact zone. Figure 9 shows the typical and representative images of the control and carbon nanotubes enhanced matrix composites. The inspection was made on the opposite side and, in this context, the blue colour represents the main damaged area promoted by the impact loads. It is possible to observe that the nanotubes incorporation seems to contribute to a slightly reduction of the damaged area, relatively to the control samples. A more detailed analysis was done measuring the damaged area (blue area) using the Image-Pro Plus software. The average values of the damaged area in terms of relative area (actual area/damaged area for control non enhanced specimen multiplied by 100) were plotted against the percentage of nanoparticles in Figure 10. As far as the control samples are concerned, the damaged area for nanoparticles enhanced matrix composites does not show a tendency of variation clearly defined, although there is a small apparent reduction. Ashrafi *et al.* [27] also obtained a small reduction of the area of impact damage (lesser than 5 %) with the incorporation of 0.1 wt% of SWCNT in carbon fiber/epoxy laminates.

The average values of the residual strength were obtained for all test conditions. The non-dimensional strength (calculated as the actual tensile strength divided by the tensile strength of non-impacted specimens) was plotted against the incident impact energy in Figures 11(a) and (b), for nanoclays and nanotubes enhanced matrix, respectively. The decay of this relative residual strength shows a reliable indicator of the damage caused by the impact. It was observed that the damage expressed by the loss of residual strength is higher for control (non-filled matrix) samples. In opposite, lower loss of residual strength was observed for the carbon nanotubes enhanced matrix laminates, which is consistent with the higher values of specific recovery energy shown previously. For 16 J incident impact energy the tensile residual strength loss is about 27, 26 and 20 % for control samples, nanoclay enhanced epoxy and carbon nanotubes

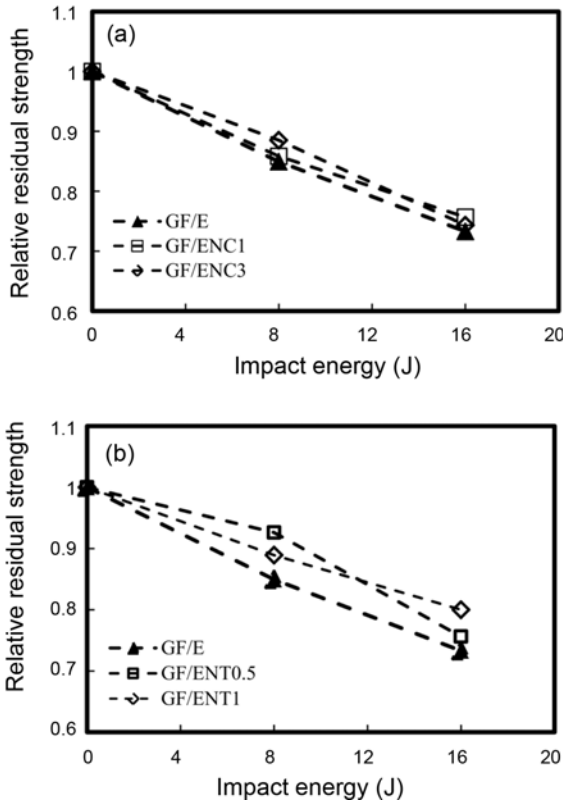

Figure 11. Non dimensional residual strength versus incident impact energy; (a) nanoclay enhanced matrix and (b) nanotubes enhanced matrix.

enhanced matrix composites, respectively. The benefit effect of nanoenhancing resin agrees with other literature works like Ashrafi *et al*. [27] which indicate an increasing of 3.5 % in compression-after-impact strength with the incorporation of 0.1 wt% of SWCNT in carbon fiber/epoxy laminates and Venkatanarayanan and Stanley [28] that obtained significant improvement on impact response of hybrid resin with MWCNT.

Conclusion

In present work it was characterized the effect of nanoclay and carbon nanotubes matrix reinforcements on low velocity impact response of epoxy/glass fiber composites concluding by small benefits with the nanoparticles incorporation. It was observed that:

1. Peak load decreases slightly with increasing percentage of nanoparticles reaching a maximum decrease of 6 % for 3 % of nanoclays.
2. Recovery energy for carbon nanotubes enhanced matrix composites is about 3-4 % higher than control samples and for nanoclay enhanced matrix laminates it is also higher, about 3 % for 8 J, but remains nearly constant for 16 J impact energy.
3. All nanoparticles enhanced matrix composites showed specific recovery energy gains in comparison with control formulation. The gain is around 14-18 % for 0.5 % wt addition of nanotubes and 7-15 % for 1 % of nanoclays, respectively, decreasing with impact energy. Specific recovery energy tends to decrease for higher percentages of nanoparticles in consequence of its poor distribution.
4. The damaged area for nanoparticles enhanced matrix composites shows no clear defined tendency, although there is a small apparent reduction. Lower impact damage quantified in terms of tensile residual strength was obtained for the carbon nanotubes enhanced matrix laminates.

Acknowledgements

The authors would like to thank Portuguese Foundation of Science and Technology for funding this work, Project n° PTDC/EME-PME/113695/2009 co-financed by FEDER, through the Operational Factors for Competitiveness Programme of the QREN with reference COMPETE: FCOMP-01-0124-FEDER-015152.

References

1. F. Rosselli and M. H. Santare, *Compos. Pt. A-Appl. Sci. Manuf.*, **28**, 587 (1997).
2. G. Caprino, *J. Compos. Mater*., **18**, 508 (1984).
3. J. C. Prichard and P. J. Hogg, *Composites,* **21**, 503 (1990).
4. G. A. O. Davies, D. Hitchings, and G. Zhou, *Compos. Pt. A-Appl. Sci. Manuf.*, **27A**, 1147 (1996).
5. S. Zheng and C. T. Sun, *Eng. Fract. Mech.,* **59**, 225 (1998).
6. M. F. S. F. Moura and A. T. Marques, *Compos. Pt. A-Appl. Sci. Manuf.*, **33**, 361 (2002).
7. R. C. Batra and N. M. Hassan, *Compos. Pt. B-Eng.,* **39**, 513 (2008).
8. R. A. Talreja in "Continuum Mechanics Characterization of Damage in Composite Materials", Vol. 399, p.195, Proc. Royal Soc. London, 1985.
9. D. Krajcinovic, and G. U. Fonseka, *J. Appl. Mech.*, **48**, 809 (1981).
10. I. Carol, E. Rizzi, and K. Willam, *Int. J. Solids Struct.*, **38**, 491 (1965).
11. B. N. Nguyen, B. J. Tucker, and M. A. Khaleel, *J. Eng. Mater. Technol.*, **127**, 337 (2005).
12. F. Meraghni, C. J. Blakeman, and M. L. Benzeggah, *Compos. Sci. Technol.*, **56**, 541 (1996).
13. N. M. Hassan and R. C. Batra, *Compos. Pt. B-Eng.,* **39**, 66 (2008).
14. R. C. Batra, G. Gopinath, and J. Q. Zheng, *Compos. Struct.*, **94**, 540 (2012).
15. A. Matzenmiller, J. Lubliner, adn R. L. Taylor, *Mech. Mater*., **20**, 125 (1995).
16. L. Weiping, V. H. Suong, and P. Martin, *Compos. Sci. Technol.,* **65**, 307 (2005).

17. X. Kornmann, R. Thomann, R. Mulhaupt, J. Finter, and L. Berlund, *J. Appl. Polym. Sci*., **86**, 2643 (2002).
18. A. J. Kinloch and A. C. Taylor, *J. Mater. Sci. Lett.*, **22**, 1439 (2003).
19. T. Yokozeki, Y. Iwahori, and S. Ishiwata, *Compos. Pt. A-Appl. Sci. Manuf.*, **38**, 917 (2006).
20. Z. Fan, M. H. Santari, and S. G. Advani, *Compos. Pt. A-Appl. Sci. Manuf.*, **39**, 540 (2008).
21. M. V. Hosur, A. A. Mohammed, S. Zainuddin, and S. Jeelani, *Compos. Struct.*, **82**, 101 (2008).
22. P. N. B. Reis, J. A. M. Ferreira, Z. Y. Zhang, T. Benameur, and M. O. W. Richardson, *Compos. Pt. B-Eng.*, **46**, 7 (2013).
23. P. N. B. Reis, J. A. M. Ferreira, Z. Y. Zhang, T. Benameur, and M. O. W. Richardson, *Compos. Pt. B-Eng.,* **56**, 290 (2014).
24. L. Ruiz-Perez, G. J. Ryston, J. P. A. Fairclough, and A. J. Ryan, *Polymer*, **49**, 4475 (2008).
25. H. Qian, E. S. Greenhalgh, M. S. P. Shaffer, and A. Bismarck, *J. Mater. Chem.*, **20**, 4751 (2010).
26. P. Ma, N. A. Siddiqui, G. Marom, and J. Kim, *Compos. Pt. A-Appl. Sci. Manuf.*, **41**, 1345 (2010).
27. B. Ashrafi, J. Guan, V. Mirjalili, Y. Zhang, L. Chun, P. Hubert, B. Simard, T. Christopher, Kingston, O. Bourne, and A. Johnston, *Compos. Sci. Technol.,* **71**, 1569 (2011).
28. P. S. Venkatanarayanan and A. Joseph Stanley, *Aerosp. Sci. Technol.,* **21**, 75 (2012).
29. H. Saghafia, R. Palazzettia, A. Zucchellia, and G. Minak, *Eng. Solid Mech.*, **1**, 85 (2013).
30. H. Çallıoglu, M. Sayer, and E. Demir, *Polym. Compos*., **32**, 1125 (2011).